Research Article | Vol. 9, No. 9 | 1 Sep 2018 | BIOMEDICAL OPTICS EXPRESS 4539
Biomedical Optics EXPRESS

Muscular blood flow responses as an early predictor of the severity of diabetic neuropathy at a later stage in streptozotocin-induced type I diabetic rats: a diffuse correlation spectroscopy study

YUMIE ONO,[1,*] KIMIYA ESAKI,[2] YUTA TAKAHASHI,[2] MIKIE NAKABAYASHI,[1,2] MASASHI ICHINOSE,[3] AND KIJOON LEE[4]

[1]*Department of Electronics and Bioinformatics, School of Science and Technology, Meiji University, 1-1-1 Higashi-Mita, Tama-ku, Kawasaki, Kanagawa 2148571, Japan*
[2]*Electrical Engineering Program, Graduate School of Science and Technology, Meiji University, 1-1-1 Higashi-Mita, Tama-ku, Kawasaki, Kanagawa 2148571, Japan*
[3]*Human Integrative Physiology Laboratory, School of Business Administration, Meiji University, 1-1 Surugadai, Kanda, Chiyoda-ku, Tokyo 1018301, Japan*
[4]*College of Transdisciplinary Studies, Daegu Gyeongbuk Institute of Science and Technology, 333 Techno Jungang-daero, Hyeonpung-myeon, Dalseong-gun, Daegu, South Korea*
**yumie@meiji.ac.jp*

Abstract: We propose a novel application of diffuse correlation spectroscopy to evaluate microvascular malfunctions of muscle tissue affected by hyperglycemia and determine their correlation with the severity of diabetic neuropathy at a later stage. Microvascular responses of the thigh muscle and the mechanical pain threshold of the hind paw of streptozotocin-induced type I diabetic rats were continuously monitored once per week for 70 days. Significantly decreased baseline blood flow and reactive hyperemia responses were observed as early as 1 week after hyperglycemia induction. The reactive hyperemia response at 2 weeks of hyperglycemia was highly correlated with the mechanical pain threshold at 8 weeks, at which time a decreased pain threshold was statistically confirmed in hyperglycemic rats relative to controls.

1. Introduction

Diabetic neuropathy is one of the most common complications of diabetes. Although diabetic neuropathy affects up to 50% of individuals with diabetes, its development is mostly asymptomatic and goes unrecognized until it becomes more advanced [1]. Diabetic sensorimotor polyneuropathy (DSPN) is a typical diabetic neuropathy that arises in the context of long-term hyperglycemia and cardiovascular risk covariates. Similar to the development of diabetic retinopathy and nephropathy, alterations of microvessels play a role in the degeneration of autonomic and sensory nerves [2]. Recent clinical research has reported the concurrence of DSPN and muscle weakness, which deteriorates the quality of life of the patient by increasing the risks of falls, immobility, and foot ulcers [3]. Therefore, early diagnosis of DSPN during the asymptomatic period is critical; however, most currently available assessments of DSPN require high-level neurophysiological laboratory settings and are limited to the direct investigation of the structure or function of neural fibers [1].

Considering the robust association between diabetic neuropathy and defective vasodilation response [4, 5], we hypothesized that changes in reactive microvascular responses may precede the development of symptomatic DSPN and be utilized as a potential predictive factor. However, the available literature on the relationship between reactive microvascular responses and the development of diabetic neuropathy is scarce due to several technical limitations. First, considerable variation in the onset duration of DSPN makes it

#332689 https://doi.org/10.1364/BOE.9.004539
Journal © 2018 Received 4 Jun 2018; revised 10 Aug 2018; accepted 16 Aug 2018; published 29 Aug 2018

Biomedical Optics EXPRESS

challenging to perform invasive blood flow measurement to track the time-course changes in rodent model experiments. Various possible mechanisms of DSPN, including advanced glycosylation end products and activation of polyol aldose reductase signaling [6], are considered to affect the heterogeneous pathophysiology of DSPN [1]. A non-invasive and repetitive measurement of tissue blood flow could be applied to track changes in tissue blood flow and its reactivity through the course of DSPN development, which varies among individuals. Second, the laser Doppler flowmeter (LDF), which is the most common technique used to non-invasively evaluate vasoreactivity changes in diabetic model animals, can only detect the blood flow responses on the surface of the skin tissue [7]. Previous reports detected deficiencies in the skin blood flow response on the scalp 1 week after induction of a diabetic state with no change in the baseline blood flow or the function and structure of the sciatic nerve [8]. A significant decrease in the baseline blood flow at the skin of the basal tail was confirmed after 4 weeks of hyperglycemic state [9]. Another group reported a significant decrease in the baseline blood flow and reactive hyperemia responses in the plantar skin of the rat hind paw after 10 weeks of diabetic state [10], after sensory deficits had been confirmed. Although these previous studies support our hypothesis, more observational time points are necessary to clearly elucidate the onset of alterations in the vasodilation response and sensory function. Moreover, measurement of blood flow in the muscle tissue is also important based on the dense distribution of capillary vessels relative to the skin tissue and the potentially earlier effect of hyperglycemia on the vasodilation response.

Therefore, we employed diffuse correlation spectroscopy (DCS) to detect microvascular responses in the thigh muscle [11] of streptozotocin (STZ)-induced type I diabetic rats. Muscle tissue was targeted owing to the dense distribution of capillary vessels and close association between muscle weakness and DSPN [3]. DCS is an optical measurement of tissue blood flow speed using the autocorrelation characteristics of near-infrared light scattered by moving red blood cells in the living body [12]. An advantage of DCS over conventional LDF is its flexibility in the depth of the measurement, which is determined by the distance between the emitter and detector optical probes [13, 14]. Numerical simulations and actual bio-optical measurements have estimated that the approximate depth of the DCS measurement below the skin surface is one-third to one-half of the inter-probe distances [13, 14]. Blood flow changes under various physiologic conditions such as reactive hyperemia and local warming/cooling tests in skin and muscle tissues have been well confirmed in our previous studies [15, 16] as well as others using simultaneous measurement of arterial spin-labeled perfusion MRI [17]. Recently developed time-domain DCS [18] has demonstrated the further potential of this diffusion optical technique to selectively measure blood flow information from a semi-arbitrary depth of the tissue with a single pair of optodes by time-gating the photon responses according to their traveling time within the tissue.

In the current study, we continuously monitored the vasodilation response of the lower limb tissue by testing post-occlusive reactive hyperemia and the mechanical pain threshold of the foot paw for 70 days. Since we observed variability in the onset duration of mechanical allodynia among the STZ-treated rats, as expected, a correlation analysis was performed to investigate which microvascular parameters in the reactive hyperemia test performed early on were predictive of the severity of DSPN observed in the later stages, as measured by the mechanical pain threshold. We specifically hypothesized that (1) hyperglycemia would alter microvascular reactivity prior to the onset of mechanical allodynia, (2) the severity of the deficit in microvascular reactivity would correspond to the degree of vascular endothelial malfunction and be correlated to the severity of the mechanical allodynia that develops in the later stage, and (3) the onset of deficits in the microvascular reactivity of muscle tissue may precede that of skin tissue based on the different capillary densities of the 2 tissues described in previous reports.

Biomedical Optics EXPRESS

2. Methods

2.1 Animals and induction of experimental diabetes

We used male Sprague-Dawley rats (6-7 weeks, weighing approximately 150 g at the beginning of the experiment) for this study. Animals were housed in groups of 2 in plexiglass cages measuring 37.1 × 23.8 × 21.6 cm and were kept in a room with controlled temperature (23 ± 3 °C) and lighting (lights on from 7:00 AM to 7:00 PM). The bedding of the cages consisted of wood shavings that were changed every 3 days for the rats in the control group throughout the experiment and prior to the induction of experimental diabetes for those in the diabetic group. The bedding of the diabetic rats was changed every day. Food and water were freely available except 12 h before the STZ or vehicle administration. This study was approved by the local Animal Care and Use Committee and conformed to the Guidelines for Care and Use of Laboratory Animals of the National Institutes of Health. Efforts were made to minimize the number of animals used as well as their suffering.

Twenty rats were fasted overnight and then made diabetic by a single intraperitoneal injection of STZ (50 mg/kg, Wako Pure Chemical Industries, Ltd.) as previously described [19]. Another 3 rats received exactly the same treatment except that they received an injection of vehicle only. A blood sample was taken 48 h after the injection from the tail vein, and blood glucose concentration was measured using a blood glucose meter (OneTouch Ultra meter, Johnson & Johnson K.K.). Seventeen out of 20 STZ-treated rats showed a blood glucose level greater than 250 mg/dL and were defined as hyperglycemic. The body weight, blood glucose concentrations, mechanical pain threshold of the hind paw, and microvascular responses for reactive hyperemia of the hind limb were recorded in all animals weekly for the following 10 weeks. Nine hyperglycemic and 1 STZ-treated normoglycemic rats did not survive the experimental period and were excluded from the analysis. Since the other STZ-treated normoglycemic rats showed comparable growth rates and blood glucose concentrations to those of the vehicle-treated rats, they were classified as controls. Therefore, data analysis was conducted with 8 diabetic and 5 control rats.

2.2 Allodynia assessment

Degeneration of sensory nerves due to long-term hyperglycemia causes diabetic neuropathy, which initially arises from hypersensitivity in the peripheral somatosensory perception of the hand and foot. The increased pain sensitivity in diabetic rats or human patients leads to mechanical allodynia, wherein pain is experienced due to a stimulus that would not normally provoke pain, such as a light touch of the skin [1, 2]. Therefore, we applied mechanical point pressure of various strengths to the paws of the rats using calibrated Von Frey filaments (Aesthesio, DanMic Global, LLC, USA) and assessed the pain threshold as a marker of mechanical allodynia in the diabetic relative to the control rats [20, 21]. Animals were placed on an elevated wire grid, and the plantar surface of the hind paw was stimulated with a series of ascending force von Frey filaments until there was a brisk paw withdrawal response. The mechanical pain threshold was interpreted as the lowest force that evoked 6 consecutive withdrawal responses. Assessments were conducted during the light phase, and pain thresholds were assessed using both sides of the hind paw. To determine the state of allodynia, the pain threshold was set at 20 g based on the average pain threshold values at which the diabetic rats showed a statistically significant withdrawal threshold relative to the control rats (19.6 g at day 56 in the current experiment) [19].

2.3 Microvascular reactivity assessment using DCS

Tissue microvascular responses for reactive hyperemia of the left thigh were assessed on a weekly basis from 2 weeks before through 10 weeks after the STZ/vehicle injection using an in-house developed DCS system [15]. In this study, we adopted 5 mm of emitter and detector separation to enable the emitted light to reach the muscle layer [22]. Rats were anesthetized

Biomedical Optics EXPRESS

with isoflurane (2.0%; 1.5 L/min) and laid on a mesh grid with their left hind limb embedded in a limb mold (Fig. 1(a)). Hairs of the left hind limb were shaved 1 day before measurement to achieve good contact of the skin surface with the DCS optical probes. The optical probes were approached to the hind limb through the optical guide embedded in the limb mold (Fig. 1(b,c)). The emitter probe (FT400EMT, Thorlabs Japan Inc., Tokyo, Japan) was connected to a long coherence, continuous red light source (DL690-050-S, 50 mW, Crysta-Laser, Reno, NV, USA), and the scattered light was detected with a photon-counting APD (tau-SPAD-50, PicoQuant, Berlin, Germany) through a single-mode operated detector probe (SM600, Thorlabs Japan Inc., Tokyo, Japan). In previous research projects, we used the 690-nm wavelength in our DCS system to enable the simultaneous measurement of DCS and near-infrared spectroscopy. However, in the present experiment, we only used the DCS system. Although the intensity of the laser was higher than the ANSI limit for human skin exposure, care has been taken to confirm that the rat skin did not experience overheating or color change after each measurement and none of the rats showed such symptoms throughout the experiment. To prevent extraneous light from contaminating the detector probe, experiments were performed in a dark room.

An in-house developed LabVIEW program collected the light intensity data from APD through a 32-bit counter board (USB-6341, National Instruments, Austin, TX, USA) at a sampling rate of 100 kS/s (kilo-sampling per second). The blood flow index (BFI), a relative value of the mean blood flow speed within a volume of the tissue through which the emitted light travels, was calculated with a fast Fourier transform-based software autocorrelator every second from the time-course of light intensity changes [23]. A detailed technical description of the DCS hardware and analysis algorithms are provided elsewhere ([12, 15]). Briefly, an autocorrelation function $G_2(r,\tau)$ of the normalized light intensity (Eq. (1)) is calculated from the detected light intensity $I(r,t)$, where r, t, τ, and brackets < > represent the position, time, the delay from t, and time-averages, respectively.

$$G_2(r,\tau) = \frac{< I(r,t) * I(r,t+\tau) >}{< I(r,t) >^2} \quad (1)$$

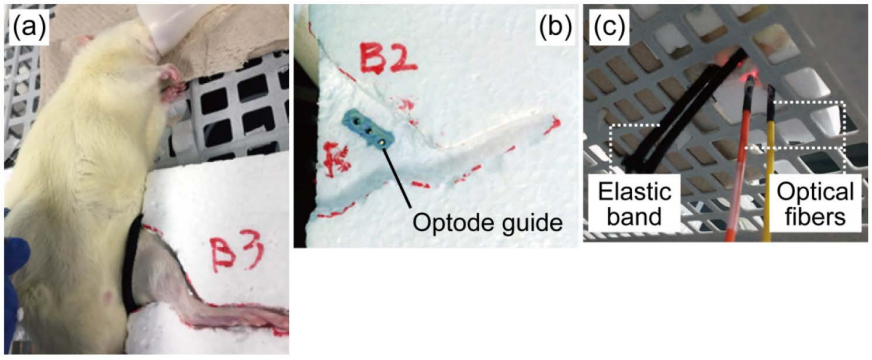

Fig. 1. Experimental setting for the reactive hyperemia test of a rat hind limb. (a) Rat is anesthetized in side lying position on the mesh grid, with its left hind limb fixed in a customized limb mold made of styrene foam. A strip of surgical tape is used to seal the limb into the mold during the DCS measurement. An elastic band is wrapped around the root of the left hind limb for occlusion. (b) A silicon optode guide is embedded in the limb mold. (c) Emitter and detector optical probes contact the skin surface through the holes of the optode guide from the bottom.

Biomedical Optics EXPRESS

To quantify the blood flow speed, $G_2(r,\tau)$ was fit to the theoretical autocorrelation function $g_2(r,\tau)$ derived from Green's function solution of the diffusion correlation equation for a point light source on the semi-infinite plate medium ([12, 15, 23]) as shown in Eq. (2):

$$g_2(r,\tau) = 1 + \beta \frac{\left| \frac{3\mu_s'}{4\pi} \left(\frac{e^{-k_D r_1}}{r_1} - \frac{e^{-k_D r_1}}{r_2} \right) \right|^2}{\langle I(r,t) \rangle^2} \tag{2}$$

where $k_D = \sqrt{3\mu_s'\mu_a + 6\mu_s'^2 k_0^2 \alpha D_B \tau}$, $r_1 = \sqrt{\rho^2 + z_0^2}$, $r_2 = \sqrt{\rho^2 + (z_0 + 2z_b)^2}$, $z_0 = \mu_s'^{-1}$, $z_b = 2(1 - R_{eff}) / 3\mu_s'(1 + R_{eff})$. Here, β is a constant, μ_s' is the reduced scattering coefficient, μ_a is the absorption coefficient, α is the fraction of photon scattering events from moving scatterers out of the total scatterers, k_0 is the wavenumber of the light in a medium, D_B is the effective diffusion coefficient of the scatterers, R_{eff} is the effective reflection coefficient, and ρ is the distance between the source and the detector. We used μ_s' = 8 cm^{-1} and μ_a = 0.03 cm^{-1}, based on the previously reported optical properties of isolated rat muscle [24] and our preliminary measurement of the optical properties of a living thigh muscle with skin layers. We defined αD_B as the BFI. The raw BFI values were presented unless otherwise stated since the hyperglycemic state strongly affected the resting state BFI values in the current experiment.

The reactive hyperemia test consisted of 1 minute of pre-occlusion rest, followed by 3 minutes of blood flow occlusion and another 6 minutes of post-occlusion rest (Fig. 2). An elastic band was wrapped around the root of the hind limb of the rat (Fig. 1(a,c)) to occlude the blood flow when pulled downward by the experimenter. The strength of the occlusion was maintained so that the BFI values during occlusion would not exceed 20% of the baseline BFI value of the pre-occlusion period. Microvascular function was evaluated with the following 5 parameters: (1) pre-occlusion, baseline mean BFI value (baseline BFI); (2) peak BFI value after the occlusion (post-occlusive reactive hyperemia (PORH) peak BFI); (3) time to PORH peak after releasing from occlusion (Tp); (4) half-decay time of the BFI value from the PORH peak (50% decay time); and (5) normalized PORH peak by dividing the peak BFI value by the baseline value. These parameters have been commonly used to study microvascular function in animal models and humans [11, 25]. The parameters measured on the first 2 days before STZ/vehicle injection were averaged and used as the baseline values (pre).

2.4 Statistical analysis

Body weight, blood glucose concentrations, mechanical pain thresholds, and microvascular responses of the reactive hyperemia test were compared using two-way repeated measures analysis of variance (ANOVA) with the factors of time and group. The normality of the data was confirmed by the Shapiro-Wilk test. The result of ANOVA was presented as F(df1, df2) = F value with their corresponding p values, where df1 and df2 indicate the degree of freedom across the group and within the group, respectively. F values were calculated to determine the main effect of each factor and the interaction of the factors. When a significant interaction of time and group factors was observed, indicating that the variables showed different time-course changes depending on the group, Tukey's post-hoc comparisons with Bonferroni correction were performed to further investigate which combination of variables across groups and/or within groups showed statistically significant differences. To further explore the microvascular responses that could facilitate the early detection of the severity of

Biomedical Optics EXPRESS

mechanical allodynia in the later stages of hyperglycemia, a correlation analysis was conducted between the individual pain threshold values at day 56, where a significant difference in the mean pain threshold was first confirmed between the control and diabetic rats and 5 microcirculation parameters of the reactive hyperemia test obtained from day 7 to day 49. Logarithms of pain threshold values were used for the correlation analysis due to a better correspondence with the microvascular responses related to the raw data. We considered $p < 0.05$ to be statistically significant.

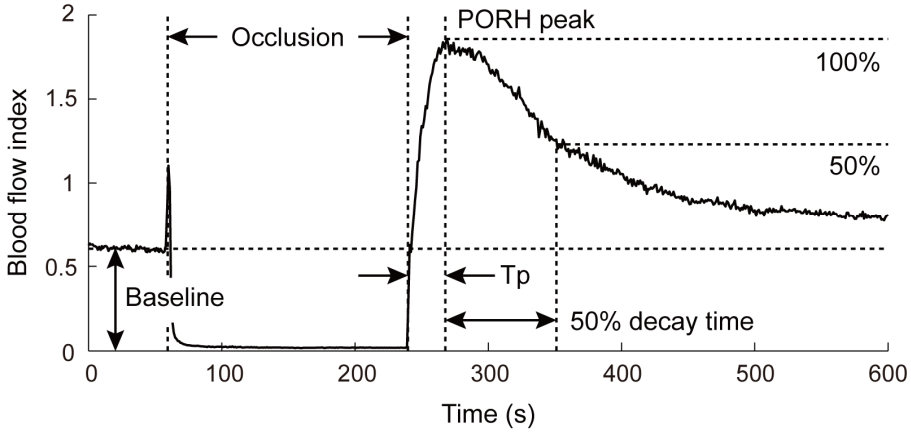

Fig. 2. Representative time-course of the blood flow index (BFI) and microvascular parameters obtained by the reactive hyperemia test. The entire test consisted of 1 minute of rest, 3 minutes of blood flow occlusion, and 6 minutes of post-occlusion rest. We evaluated the mean BFI value at rest (baseline), peak BFI value after releasing from occlusion (post-occlusive reactive hyperemia (PORH) peak), time to PORH peak after releasing from occlusion (Tp), and half-decay time from the PORH peak (50% decay time). Normalized PORH peaks were also calculated by dividing the peak BFI value by the baseline value.

Biomedical Optics EXPRESS

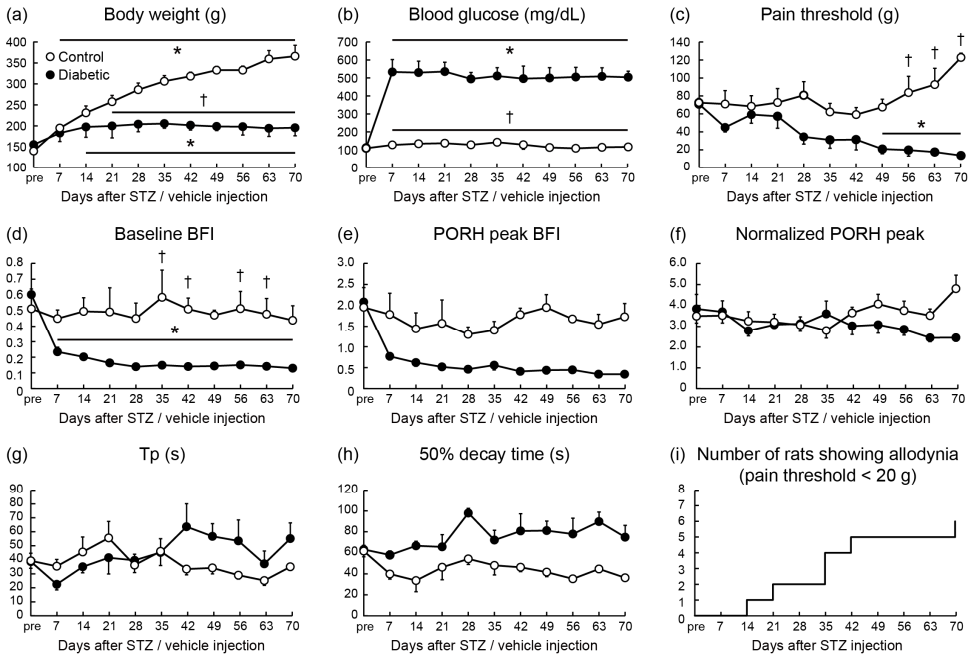

Fig. 3. Changes in the (a) body weight, (b) blood glucose concentrations, (c) mechanical pain thresholds, (d-h) microvascular responses to the reactive hyperemia test, and (i) cumulative number of diabetic rats showing allodynia throughout the experimental period in control and diabetic rats. Data obtained in the first 2 measurements prior to the STZ/vehicle administration were averaged and used as baseline values (pre). Error bars show standard errors. The asterisk (*) indicates statistically significant changes from pre. The dagger (†) indicates a statistically significant difference between the control and diabetic rats at the corresponding time period. BFI: blood flow index, PORH: post-occlusive reactive hyperemia, Tp: time to peak.

3. Results

Time-course changes in the mean body weight, blood glucose concentrations, mechanical pain thresholds, and microvascular responses of the reactive hyperemia test are summarized in Fig. 3. The mean BFI time-courses during the reactive hyperemia test were superimposed across the experimental time periods and are shown in Fig. 4. Although control rats showed a mostly constant response pattern throughout the entire experimental period, diabetic rats showed an almost immediate decline in the baseline BFI and reactive hyperemia responses after the induction of experimental diabetes. Statistical results for each specific parameter are described in the following paragraphs.

3.1 Body weight and blood glucose concentrations

Figures 3(a) and 3(b) show the changes in the body weight and blood glucose concentrations of the animals. There was a statistically significant main effect of group and time in addition to a significant interaction between group and time for both measures (group vs. time interaction: $F(10,121) = 34.53$ and 19.98 in body weight and blood glucose concentration, respectively, $p < 0.001$). Both the control and diabetic rats showed a statistically significant increase in body weight compared to the baseline period. However, the statistical significance developed 1 week earlier in the control rats compared to the diabetic rats. We also found a statistically significant increase in the body weight of the control rats relative to diabetic rats from 3 weeks after the STZ/vehicle injection to the end of the experiment (Fig. 3(a)). Blood glucose concentrations of the rats in the diabetic group were significantly increased after the induction of experimental diabetes relative to the concentrations in the baseline and those of the control rats, which were maintained throughout the experimental period (Fig. 3b). The

Biomedical Optics EXPRESS

impaired growth rate and highly maintained blood glucose concentrations are typical characteristics of diabetic animals.

3.2 Pain threshold

Figure 3(c) shows the changes in the mechanical pain threshold of the left hind paw. There was a significant main effect of group ($F(1,121) = 78.44$, $p < 0.001$) and an interaction between group and time ($F(10,121) = 4.27$, $p < 0.001$). Despite the rapid increase in blood glucose concentrations in the diabetic rats, the onset of mechanical allodynia was relatively late. A statistically significant decrease in the pain threshold of the diabetic rats relative to the baseline threshold values was first confirmed at day 49 and maintained significant until the end of the experimental period ($p < 0.05$). A statistically significant difference in the pain threshold between control and diabetic rats was found from day 56 to the end of the experiment ($p < 0.05$). The pain threshold of the right hind paw also showed a significant decrease in the diabetic rats relative to the control rats from day 56 to the end of the experiment ($F(10,121) = 3.80$, $p < 0.001$; data not shown), confirming that the STZ administration well mimicked the symmetrical and length-dependent pathophysiology of DSPN [2]. Figure 3i indicates the cumulative number of diabetic rats that showed pain threshold values of less than 20 g throughout the experimental period, which reveals a considerable variety in the onset time of mechanical allodynia. Although the statistically significant group difference in the pain threshold did not appear until day 56, half of the diabetic rats showed allodynia by day 35.

3.3 Microvascular responses

Hyperglycemia immediately decreased the baseline BFI in the diabetic rats (Figs. 3(d) and 4), which was statistically significant from day 7 throughout the experiment. Significant group differences were found on days 35, 42, 56, and 63 (main effect in group: $F(1,121) = 107.09$, $p < 0.001$; main effect in time: $F(10,121) = 2.55$, $p < 0.01$; and group vs. time interaction: $F(10,121) = 2.18$, $p = 0.023$). PORH peak BFI also decreased in the diabetic rats with a significant main effect with respect to the group ($F(1,121) = 83.36$, $p < 0.001$), though the interaction between the group and time was not statistically significant (Fig. 3(e); group vs. time interaction: $F(10,121) = 1.87$, $p = 0.056$). Accordingly, the normalized PORH peak was comparable throughout the experimental period (Fig. 3(f)). Although Tp tended to increase in the diabetic rats in the later stages of hyperglycemia, neither a main effect nor an interaction was observed (Fig. 3(g)). There was a main group effect in the 50% decay time ($F(1,121) = 13.72$, $p < 0.001$), but no interaction between time and group (Fig. 3(h)). The lack of any time and group interactions in the microvascular responses aside from baseline BFI might be due to the widely distributed onsets of allodynia (Fig. 3(i)).

Biomedical Optics EXPRESS

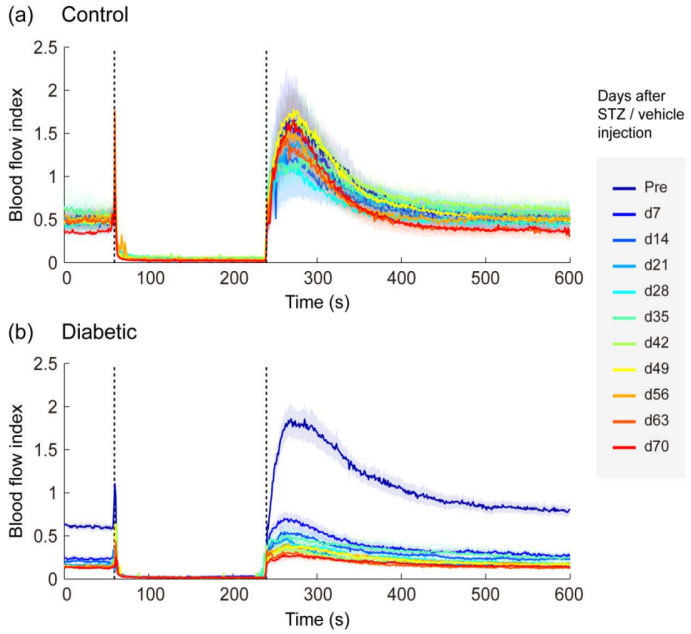

Fig. 4. Superimposed time trace of the blood flow index (BFI) during reactive hyperemia testing in rats in the control (a) and diabetic (b) groups across different experimental days. Vertical dotted lines show durations of occlusion. Solid lines show mean values, and shaded areas show standard errors.

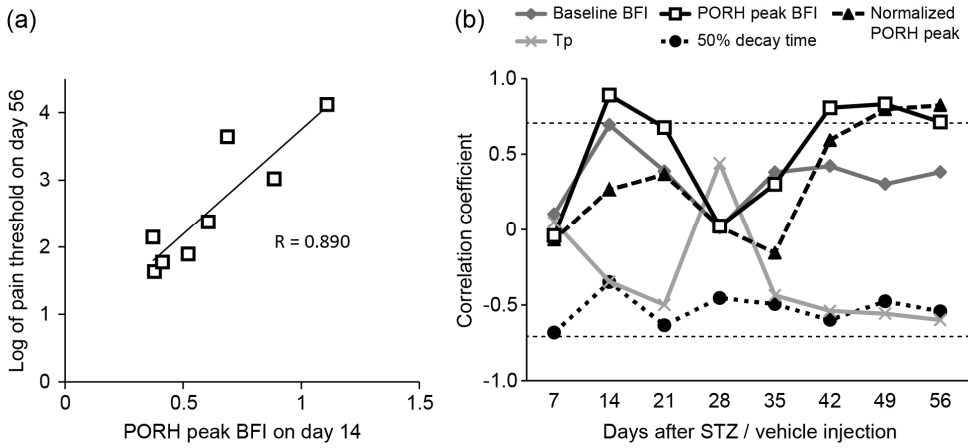

Fig. 5. Correlations between microvascular responses during reactive hyperemia testing in the early stage of hyperglycemia and the severity of diabetic neuropathy during the later stages. (a) Relationship between the PORH peak BFI in the diabetic rats on day 14 and the logarithm of mechanical pain thresholds on day 56, which showed the highest correlation coefficient among the combinations tested. (b) Summary of the correlation coefficients between microvascular responses on each experimental day and the logarithm of mechanical pain thresholds on day 56. Horizontal dotted lines show the correlation coefficient values with statistical significance ($p<0.05$) based on the number of subjects. BFI: blood flow index, PORH: post-occlusive reactive hyperemia, Tp: time to peak.

Biomedical Optics EXPRESS

3.4 Early microvascular responses predicting the severity of DSPN during the later stages

The microvascular responses of baseline BFI, PORH peak BFI, and normalized PORH peak tended to positively correlate with the severity of diabetic neuropathy in the later stage (Fig. 5). Conversely, Tp and 50% decay time tended to show a negative correlation. A statistically significant correlation was observed in the PORH peak BFI on days 14, 42, 49, and 56 and in the normalized PORH peak on days 49 and 56. The highest correlation was observed in the PORH peak BFI on day 14 ($r = 0.890$, $p = 0.003$).

4. Discussion

This study investigated the development of mechanical allodynia in STZ-induced type I diabetic rats and its relationship with microvascular reactivity. A simulated hyperglycemic state rapidly decreased the resting-state peripheral blood flow relative to the baseline within 1 week, which was later confirmed by the statistically significant decrease relative to that in the normoglycemic group at week 5. Since the decrease in the mechanical pain threshold in the diabetic rats became significant after the aforementioned dysfunction in peripheral blood flow, the current results support the hypothesis that the early-developed endothelial dysfunction in the hyperglycemic state [8] may cumulatively affect the peripheral sensory nerves and lead to the development of mechanical allodynia in the later stages. The novel finding is that the severity of the decrease in blood flow reactivity in an early stage of hyperglycemia is positively correlated with the severity of the mechanical allodynia in a later stage, suggesting a possible use of blood flow reactivity for the early prediction of the prognosis of DSPN. The non-invasive measurement of blood flow reactivity using DCS enabled the repetitive screening of the same animal to track individual differences in peripheral blood flow reactivity under hyperglycemic conditions.

A comparison of the current results with those of previous reports using LDF further revealed the difference in the onset of vascular response deficits between the muscle and skin tissues. Baseline blood flow of the basal tail skin remained comparable to that at pre-STG administration until 4 weeks after induction of a hyperglycemic state [9], while that of the thigh muscle showed significant decreases relative to the pre-STG administration baseline within only 1 week. Since the onset of sensory dysfunction determined from the behavior test is comparable between the current study and the previous literature (7 weeks [10]), these results suggest a tissue-dependent effect of the hyperglycemic state on the blood flow. Cameron et al. [26] reported the rapid reduction of endoneurial blood flow in the sciatic nerve by 41.2% compared with that in the onset controls as early as 1 week after the induction of a diabetic state. The current blood flow measurement of the thigh muscle showed greater restriction of the baseline blood flow by 61.1% at 1 week after STZ treatment. Increased blood viscosity [26] and/or leukocyte-capillary plugging [27] are possible mechanisms of the elevated vascular resistance and decreased blood flow in diabetic rats. Although further investigation is required to elucidate the physiological mechanism of variable tolerance to the hyperglycemic state among tissue types, our results demonstrated that muscle blood flow is more susceptible to hyperglycemic stress relative to skin blood flow. Therefore, DCS is a potentially superior option over LDF for the early detection of abnormal microvascular function. Further studies with DCS using different inter-probe distances to monitor both the skin and muscle blood flows may confirm the tissue-dependent effect of the hyperglycemic state on blood flow.

The hyperglycemic state also affected the parameters of microvascular reactivity in the reactive hyperemia test. Statistically significant group main effects were found in the PORH peak BFI and 50% decay time. The decreased post-occlusive peak blood flow and prolonged 50% decay time indicate endothelial dysfunction due to hyperglycemia, which appeared as early as 1 week post-STZ-treatment and persisted throughout the experimental period. In contrast, a gradual prolongation of the Tp of diabetic rats was observed in the later stages of

Biomedical Optics EXPRESS

hyperglycemia, which suggests that multiple mechanisms [1,6] affect the reactive hyperemia response in diabetic rats.

According to the correlation analysis between the microvascular response parameters and the severity of diabetic neuropathy during the later stages of hyperglycemia, the PORH peak BFI on day 14 showed the highest correlation with the later-stage severity of diabetic neuropathy. Although not statistically significant, the 50% decay time and baseline BFI also showed a medium-to-high correlation with the later severity of diabetic neuropathy. Of importance is the fact that on day 14, almost all diabetic rats were asymptomatic of DSPN (7 out of 8 rats showed a pain threshold above 20 g). Predicting the future severity of DSPN during such an asymptomatic period would have a significant clinical impact in terms of educating patients and motivating them for treatment. Interestingly, some parameters including PORH peak BFI and baseline BFI showed a dip in the correlation coefficient in the middle of the experimental period (days 28 and 35). This finding suggests a late onset of various pathological alterations that transiently affected the blood flow and its response. The mechanisms underlying DSPN are considered to be multifactorial [28], the various combinations of which are likely to yield heterogeneous pathophysiology [1]. In addition, the accelerated increase in the number of diabetic rats showing allodynia after day 35 supports the continued progression of the pathological state after that period.

Notably, the detection capability of the reactive hyperemia test parameters may become less reliable as the BFI value decreases in the later stage in diabetic animals and as the detected values are more susceptible to intrinsic fluctuations in the BFI values due to blood flow changes related to the cardiac cycle [29]. Future studies should apply the simultaneous measurement of pulse wave and photon intensity to accurately determine the BFI in either the diastolic or systolic phase. Another limitation of this study is a relatively low sampling frequency of photon counting signals due to the technical limitation of the acquisition software, which may have underestimated the PORH peak BFI values especially in the control rats. Improving the sampling frequency of the system may further disclose the significant differences in PORH peak characteristics between the control and diabetic rats. Although during occlusion, the parameters of the reactive hyperemia test and the ratio of BFI values relative to the baseline in the control rats showed no statistically significant correlation (data not shown; can be shared upon request), the variation in occlusal strength should be further minimized to obtain accurate reactive vascular responses.

In conclusion, we proposed a novel application of DCS to enable the early detection of the severity of DSPN during the asymptomatic stages. In vivo blood flow measurement of pharmacologically-induced diabetic rats revealed very early changes in microvascular function due to hyperglycemia, before the onset of mechanical allodynia. The peak response in the reactive hyperemia test in the early stage of hyperglycemia significantly correlated with the severity of the pain threshold in the later stages, which suggests a relationship between the degree of vascular endothelial malfunction and symptom progression in DSPN. A comparison of the current results with those from previous LDF studies further validated the advantage of the DCS measurement of muscle blood flow to detect microvascular malfunctions earlier than when using skin blood flow measurements. The relatively compact experimental setting of DCS may further contribute to the early, non-invasive, and cost-effective diagnosis of microvascular dysfunction in patients with diabetes. Going forward, concurrent DCS measurement of both shallow and deep tissues during static and exercise conditions in human patients may aid the elucidation of the microcirculatory mechanisms of muscle weakness in DSPN.

Funding

JSPS KAKENHI (Grant Number JP 16H03242).

Biomedical Optics EXPRESS

Acknowledgments

The authors thank Professor Chen-Tung Yen Ph. D., Hsiao-Chun Lin, Ph. D. (National Taiwan University, Taiwan), Taro Taguchi, M.S., and Ryohei Ouchi, B.S. (Meiji University, Japan) for their valuable support in the preparation of the diabetic model rats.

Disclosures

The authors declare that there are no conflicts of interest related to this article.

References

1. P. R. Vas, S. Sharma, and G. Rayman, "Distal sensorimotor neuropathy: improvements in diagnosis," Rev. Diabet. Stud. **12**(1-2), 29–47 (2015).
2. S. Tesfaye, A. J. Boulton, P. J. Dyck, R. Freeman, M. Horowitz, P. Kempler, G. Lauria, R. A. Malik, V. Spallone, A. Vinik, L. Bernardi, and P. Valensi; Toronto Diabetic Neuropathy Expert Group, "Diabetic neuropathies: update on definitions, diagnostic criteria, estimation of severity, and treatments," Diabetes Care **33**(10), 2285–2293 (2010).
3. H. Andersen, "Motor dysfunction in diabetes," Diabetes Metab. Res. Rev. **28**(1), 89–92 (2012).
4. A. Veves, C. M. Akbari, J. Primavera, V. M. Donaghue, D. Zacharoulis, J. S. Chrzan, U. DeGirolami, F. W. LoGerfo, and R. Freeman, "Endothelial dysfunction and the expression of endothelial nitric oxide synthetase in diabetic neuropathy, vascular disease, and foot ulceration," Diabetes **47**(3), 457–463 (1998).
5. N. E. Cameron, S. E. M. Eaton, M. A. Cotter, and S. Tesfaye, "Vascular factors and metabolic interactions in the pathogenesis of diabetic neuropathy," Diabetologia **44**(11), 1973–1988 (2001).
6. J. W. Albers and R. Pop-Busui, "Diabetic neuropathy: mechanisms, emerging treatments, and subtypes," Curr. Neurol. Neurosci. Rep. **14**(8), 473 (2014).
7. R. Bi, J. Dong, C. L. Poh, and K. Lee, "Optical methods for blood perfusion measurement--theoretical comparison among four different modalities," J. Opt. Soc. Am. A **32**(5), 860–866 (2015).
8. D. Sigaudo-Roussel, C. Demiot, B. Fromy, A. Koïtka, G. Lefthériotis, P. Abraham, and J. L. Saumet, "Early endothelial dysfunction severely impairs skin blood flow response to local pressure application in streptozotocin-induced diabetic mice," Diabetes **53**(6), 1564–1569 (2004).
9. M. S. Rendell, S. T. Kelly, D. Finney, T. Luu, K. Kahler, S. F. McIntyre, and J. V. Terando, "Decreased skin blood flow early in the course of streptozotocin-induced diabetes mellitus in the rat," Diabetologia **36**(10), 907–911 (1993).
10. X. Y. Yang, L. Sun, P. Xu, L. L. Gong, G. F. Qiang, L. Zhang, and G. H. Du, "Effects of salvianolic scid A on plantar microcirculation and peripheral nerve function in diabetic rats," Eur. J. Pharmacol. **665**(1-3), 40–46 (2011).
11. R. Cheng, X. Zhang, A. Daugherty, H. Shin, and G. Yu, "Noninvasive quantification of postocclusive reactive hyperemia in mouse thigh muscle by near-infrared diffuse correlation spectroscopy," Appl. Opt. **52**(30), 7324–7330 (2013).
12. T. Durduran, R. Choe, W. B. Baker, and A. G. Yodh, "Diffuse optics for tissue monitoring and tomography," Rep. Prog. Phys. **73**(7), 076701 (2010).
13. M. S. Patterson, S. Andersson-Engels, B. C. Wilson, and E. K. Osei, "Absorption spectroscopy in tissue-simulating materials: a theoretical and experimental study of photon paths," Appl. Opt. **34**(1), 22–30 (1995).
14. G. Yu, T. Durduran, G. Lech, C. Zhou, B. Chance, E. R. Mohler 3rd, and A. G. Yodh, "Time-dependent blood flow and oxygenation in human skeletal muscles measured with noninvasive near-infrared diffuse optical spectroscopies," J. Biomed. Opt. **10**(2), 024027 (2005).
15. M. Nakabayashi and Y. Ono, "Detection of Blood Flow Speed in Shallow and Deep Tissues Using Diffuse Correlation Spectroscopy," Advanced Biomedical Engineering **6**(0), 53–58 (2017).
16. M. Ichinose, M. Nakabayashi, and Y. Ono, "Sympathoexcitation constrains vasodilation in the human skeletal muscle microvasculature during post-occlusive reactive hyperemia," Am. J. Physiol. Heart Circ. Physiol. **315**(2). H242–H253 (2018).
17. G. Yu, T. F. Floyd, T. Durduran, C. Zhou, J. Wang, J. A. Detre, and A. G. Yodh, "Validation of diffuse correlation spectroscopy for muscle blood flow with concurrent arterial spin labeled perfusion MRI," Opt. Express **15**(3), 1064–1075 (2007).
18. M. Pagliazzi, S. K. V. Sekar, L. Colombo, E. Martinenghi, J. Minnema, R. Erdmann, D. Contini, A. D. Mora, A. Torricelli, A. Pifferi, and T. Durduran, "Time domain diffuse correlation spectroscopy with a high coherence pulsed source: in vivo and phantom results," Biomed. Opt. Express **8**(11), 5311–5325 (2017).
19. T. J. Morrow, "Animal models of painful diabetic neuropathy: the STZ rat model," Curr. Protoc. Neurosci. **9**(1), 18 (2004).
20. G. J. Bennett, J. M. Chung, M. Honore, and Z. Seltzer, "Models of neuropathic pain in the rat," Curr. Protoc. Neurosci. **9**(1), 14 (2003).
21. M. Wei, L. Ong, M. T. Smith, F. B. Ross, K. Schmid, A. J. Hoey, D. Burstow, and L. Brown, "The streptozotocin-diabetic rat as a model of the chronic complications of human diabetes," Heart Lung Circ. **12**(1), 44–50 (2003).

Biomedical Optics EXPRESS

22. T. Iwaki, H. Yamashita, and T. Hayakawa, *A Color Atlas of Sectional Anatomy of the Rat.* (Adthree Publishing, 2001).
23. J. Dong, R. Bi, J. H. Ho, P. S. Thong, K. C. Soo, and K. Lee, "Diffuse correlation spectroscopy with a fast Fourier transform-based software autocorrelator," J. Biomed. Opt. **17**(9), 097004 (2012).
24. B. Beauvoit, S. M. Evans, T. W. Jenkins, E. E. Miller, and B. Chance, "Correlation between the light scattering and the mitochondrial content of normal tissues and transplantable rodent tumors," Anal. Biochem. **226**(1), 167–174 (1995).
25. R. Yamamoto-Suganuma and Y. Aso, "Relationship between post-occlusive forearm skin reactive hyperaemia and vascular disease in patients with Type 2 diabetes-a novel index for detecting micro- and macrovascular dysfunction using laser Doppler flowmetry," Diabet. Med. **26**(1), 83–88 (2009).
26. N. E. Cameron, M. A. Cotter, and P. A. Low, "Nerve blood flow in early experimental diabetes in rats: relation to conduction deficits," Am. J. Physiol. **261**(1), E1–E8 (1991).
27. A. G. Harris, T. C. Skalak, and D. L. Hatchell, "Leukocyte-capillary plugging and network resistance are increased in skeletal muscle of rats with streptozotocin-induced hyperglycemia," Int. J. Microcirc. Clin. Exp. **14**(3), 159–166 (1994).
28. A. M. Vincent, B. C. Callaghan, A. L. Smith, and E. L. Feldman, "Diabetic neuropathy: cellular mechanisms as therapeutic targets," Nat. Rev. Neurol. **7**(10), 573–583 (2011).
29. D. Wang, A. B. Parthasarathy, W. B. Baker, K. Gannon, V. Kavuri, T. Ko, S. Schenkel, Z. Li, Z. Li, M. T. Mullen, J. A. Detre, and A. G. Yodh, "Fast blood flow monitoring in deep tissues with real-time software correlators," Biomed. Opt. Express **7**(3), 776–797 (2016).